SHAPE OF THE SUBSONIC PART OF A NOZZLE WITH A FLAT ACOUSTIC SURFACE WITH ALLOWANCE FOR VISCOSITY IN THE BOUNDARY-LAYER APPROXIMATION

I. L. Osipov, A. V. Shipilin, and N. P. Shulishnina

UDC 532.526

A numerical construction is proposed for the shape of the wall of the subsonic part of a nozzle. The design realizes nonseparated flow with an absence of local supersonic zones. The method is based on the simultaneous numerical solution of boundary-layer equations and equations of motion of an inviscid gas.

The task of profiling is broken down into successive stages. First, a solution is obtained for the inverse problem of designing the subcritical part of the nozzle for inviscid flow, with data being assigned on a previously unknown wall of the nozzle AB (Fig. 1). Then design curve AB is taken as the outer boundary of the boundary layer formed near the nozzle wall, and the second stage of the solution is begun. This stage consists of calculating the equations of the boundary layer and the displacement thickness, which is then used to determine the corrected nozzle wall AQ (Fig. 1).

Let us examine the first problem. A distribution of Mach numbers $M = M(s) \leqslant 1$ is given along a curve AB of length l (Fig. 1). It is assumed that the size of the inlet aperture AD is given, while the condition $M = 1$ must be satisfied at the outlet BC. The condition $V_y = 0$ must be satisfied at AD and on the symmetry axis DC. Flow is assumed to be inviscid and eddy-free in the region ABCD and described by the equations:

$$\frac{\partial}{\partial x}(y^{\nu}\rho V_x) + \frac{\partial}{\partial y}(y^{\nu}\rho V_y) = 0, \quad \frac{\partial V_x}{\partial y} = \frac{\partial V_y}{\partial x},$$
$$\frac{w^2}{2} + \frac{\varkappa P}{(\varkappa - 1)\rho} = C_1, \quad \frac{P}{\rho^{\varkappa}} = C_2, \quad w^2 = V_x^2 + V_y^2, \tag{1}$$

where $\nu = 0$ and 1 for the two-dimensional and axisymmetric cases, respectively.

This problem is solved numerically using the iteration method described in [1]. After the first problem is solved, the coordinates of the curve AB and θ – the slope of the velocity vector to the x axis – are determined.

Between the nozzle wall AQ (Fig. 1) and the curve AB, we assume the flow to be viscous and to satisfy the equations of a laminar compressible boundary layer:

$$\rho u\frac{\partial u}{\partial s} + \rho v\frac{\partial u}{\partial n} = -\frac{\partial P_e}{\partial s} + \frac{\partial}{\partial n}\left(\mu\frac{\partial u}{\partial n}\right),$$
$$\frac{\partial}{\partial s}[r^{\nu}(s)\rho u] + \frac{\partial}{\partial n}[r^{\nu}(s)\rho v] = 0,$$
$$\rho u\frac{\partial h}{\partial s} + \rho v\frac{\partial h}{\partial n} = \frac{\partial}{\partial n}\left(\frac{\mu}{\mathrm{Pr}}\frac{\partial h}{\partial n}\right) - \frac{\partial}{\partial n}\left[\left(\frac{1}{\mathrm{Pr}} - 1\right)\mu\frac{\partial (u^2/2)}{\partial n}\right], \tag{2}$$
$$h = \frac{\varkappa P}{(\varkappa - 1)\rho} + \frac{u^2}{2}.$$

Equations (2) are written in orthogonal coordinates s and n, related to the surface of the wall.

Computer Center of the Academy of Sciences of the USSR, Moscow. Translated from Inzhenerno-Fizicheskii Zhurnal, Vol. 42, No. 5, pp. 724-729, May, 1982. Original article submitted March 9, 1981.

0022-0841/82/4205-0491$07.50

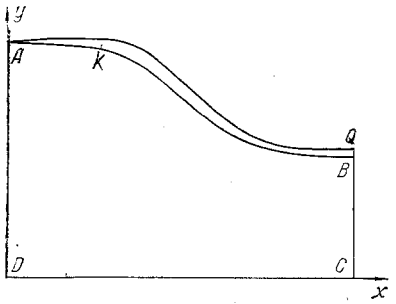

Fig. 1. Flow region in the variables x, y.

The boundary conditions have the form

$$u(s,\ 0) = v(s,\ 0) = 0, \quad u(s,\ \infty) = w_e(s),$$

$$h(s,\ 0) = \frac{\varkappa}{\varkappa - 1} RT_w(s), \quad h(s,\ \infty) = h_e(s).$$

The pressure P_{e0} and temperature T_{e0} are assigned at point A. These values and the quantity M(0) are used to calculate the constants C_1 and C_2 in Eq. (1). Along AB we have

$$w_e(s) = \sqrt{2C_1(\varkappa - 1)M^2(s)/[2 + (\varkappa - 1)M^2(s)]},$$

$$h_e(s) = C_1,\ P_e(s) = C_2\left[\frac{\varkappa - 1}{2\varkappa}\ \frac{2C_1 - w_e^2}{2}\right]^{\frac{\varkappa}{\varkappa - 1}}. \tag{3}$$

In the axisymmetric case, r(s) is given in the form of a table obtained from calculating inviscid flow. In the numerical integration of system (2), it is assumed that there is no boundary layer at point A. The boundary conditions at s = 0 were obtained by solving the similar problem of the boundary layer on a plate.

System (2) was integrated numerically using the finite-difference method proposed in [2]. The method is based on a difference representation of the boundary-layer equations written in integral form.

The displacement thickness δ^* is calculated as a function of s after the boundary-layer equations are integrated. Knowing x and r — the coordinates of the curve AB — and the quantities ϑ and δ^*, the formulas

$$\bar{r} = r + \delta^* \cos(\vartheta), \quad \bar{x} = x - \delta^* \sin(\vartheta) \tag{4}$$

can be used to calculate the coordinates $\bar{x}$ and $\bar{r}$ of the corrected nozzle wall.

The number of design points for solving the first problem was 400 (10 along the y axis and 40 along the x axis), while the second problem was solved using 500 points along the n axis and 400 points along the s axis. The average computing time for one variant on a BÉSM-6 computer was 30 min.

Figure 2 shows examples of calculated contours for axisymmetric nozzles. The following Mach number distribution was selected for curves 1 and 2 along AB:

$$M^2(s) = M_0^2 + (1 - M_0^2)\exp[-K(s - L)^2]. \tag{5}$$

Integration of the boundary layer in these and subsequent calculations was done under the following conditions: the value of T_{e0} was taken at 1500°K, pressure P_{e0} = 1 atm, and the temperature of the nozzle wall T_W was a constant 373°K. The length of the generatrix L = 2, the viscosity coefficient was determined from Sutherland's equation, and the Prandtl number Pr = 0.71.

Figure 3a shows corresponding values of $m^* = \delta^*\sqrt{\mathrm{Re}}/(r_A s)$ in relation to s for the nozzles shown in Fig. 2. It is apparent that the displacement thickness is relatively small for all values of s. The transsonic parts of the inviscid and corrected nozzles differ very little, especially for the steeper nozzle (curve 2). Since, in accordance with Eqs. (5) and (3), pressure decreases monotonically along AB in these variants, boundary-layer separation does not occur.

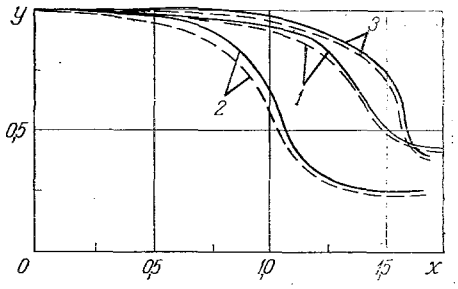

Fig. 2. Contours of nozzles constructed without allowance for viscosity (dashed curves) and corrected with Eqs. (4) (solid curves). The values of M(s) were given from Eq. (5) for curves 1 and 2: 1) at $M_0^2 = 0.01$, K = 13.5; 2) at $M_0^2 = 0.001$, K = 8; 3) values of M(s) given from Eq. (6) (variant 6 from Table 2).

TABLE 1. The Relation σ(K, L) with M(s) Given from Eq. (5)

K	13,5	13,5	13,5	36	54	67,5	94,5
L	2	2,167	2,333	2	2	2	2
σ, %	10,5	7,1	4,5	8,0	7,3	7,4	7,6

However, the calculated gas flow in the above nozzles at the inlet section AD is nonuniform with respect to the velocity modulus of w. It should be noted that the uniformity of the flow is guaranteed in the present work by the formulation of the problem. The condition of flow uniformity at the outlet is of practical interest in design work, such as for wind tunnels or gas-discharge and ion lasers [3, 4]. However, works devoted to obtaining a uniform outflow also presuppose uniformity at the inlet, owing to design considerations. Therefore, it is interesting to determine which factors will yield a uniform flow at the inlet given a uniform outflow.

The degree of nonuniformity of the inflow may be characterized by the parameter $\sigma = \Delta w / w_A \times 100\%$, where $\Delta w = \max|w - w_A|$ among all of the values of velocity modulus taken along AD. Calculations showed that $\Delta w = w_D - w_A$ for nozzles with a monotonic distribution of velocity along AB, such as given by Eq. (5). The value of σ increases with an increase in the steepness of the nozzle walls. For the nozzle represented by curve 1 in Fig. 2, σ = 10.5%. For the steeper nozzle represented by curve 2, σ = 17.1%.

One method of obtaining a uniform flow at the inlet is increasing the nozzle length with a fixed value of M_0 at point A. Thus, it can be seen from Table 1 that, for the velocity distribution (5) being examined, lengthening of L by 0.167, i.e., by ∼8%, lowers σ from 10.5 to 7.1%. An increase in L by 0.333 decreases σ to 4.5%. But lengthening the generatrix of the nozzle leads to an unwanted increase in its weight. Therefore, it would be useful to solve the problem of reducing the nonuniformity of the inflow with fixed values of M_0 and L. It should be noted that a similarly stated problem was studied in [3], which dealt with subsonic channels. In this work, flow nonuniformity was decreased as a result of selection of the nozzle wall by solving a series of direct problems.

In our work, flow nonuniformity is decreased by selecting an appropriate velocity distribution along the outer boundary of the boundary layer (Fig. 1). By increasing the size of the nearly straight section AK (Fig. 1), we can decrease σ. For distribution (5), an increase in the section AK with a fixed length of curve AB is achieved by increasing the value of the parameter K. The dependence of σ on K is shown in Table 1. An increase in K from 13.5 to 54 reduces σ to 7.3%. However, a further increase in K not only fails to further reduce σ, but increases it. This has to do with the fact that, at high K, the contour corresponding to inviscid flow becomes so steep that V_x becomes negative close to the wall.

Another, more effective method of reducing σ is selecting a nonmonotonic velocity distribution along the wall. The following distribution was used in calculations:

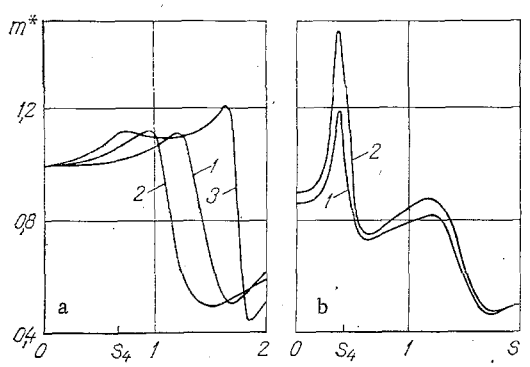

Fig. 3. Dependence of dimensionless displacement thickness m^* on length of contour s: a) for nozzles 1-3, shown in Fig. 2; b) for nozzles with the M(s) distribution given by Eq. (6) (variant 1 from Table 2) at values of T_{e0} equal to 4000°K (curve 1) and 3000°K (2).

$$M^2(s) = \begin{cases} M_0^2 + (M_1^2 - M_0^2)\exp[-K_1(s-s_2)^2], & s < s_1, \\ m(s-s_1)^3 + n(s-s_1)^2 + M_1^2, & s_1 \leqslant s \leqslant s_2, \\ M_0^2 + (1-M_0^2)\exp[-K(s-L)^2], & s > s_2, \end{cases} \tag{6}$$

where $0 < M_1^2 < M_0^2$, $0 < s_1 < s_2 < L$. The coefficients m and n are chosen from the condition of joining of the functions M^2 and dM/ds at point s_2. At $s > s_2$, Eq. (6) agrees with Eq. (5). The form of the function M(s) given by Eq. (6) is shown in Fig. 4 for two different sets of values of the parameters s_1, s_2, M_1, and K_1.

The derivative dM/ds is negative at $s < s_1$. Introduction of the wall section on which velocity decreases allows us to reduce σ. It should be noted that, in this case, Δw is no longer equal to the difference $w_D - w_A$. Regarding inviscid flow, by selecting four free parameters in the distribution (6) — s_1, s_2, M_1, and K_1 — we can reduce σ to any fixed value. Thus, Table 2 shows values of the parameters at which $\sigma \leq 1.2\%$ in variants 2-6.

However, if the function M(s) — thus, the pressure along the outer boundary of the boundary layer AB — is nonmonotonic, the lack of boundary-layer separation can no longer be guaranteed. Nevertheless, by calculating the boundary-layer equation, we can not only determine a correction for the resulting contour, but also check to ensure the absence of separated flow

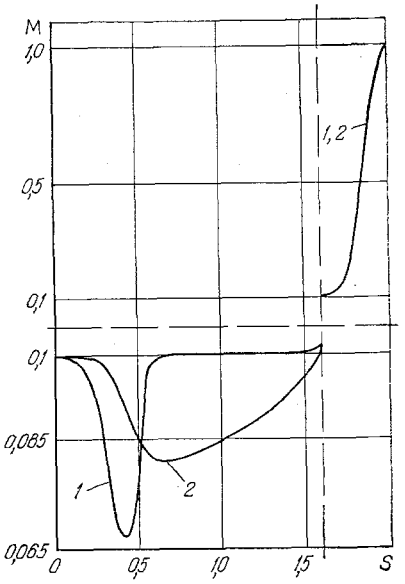

Fig. 4. The relation M(s), calculated from Eq. (6), for different values of the parameters s_1, s_2, M_1, and K_1: 1) results corresponding to the first column in Table 2; 2) results for the sixth column.

TABLE 2. Values of the Parameters in Eq. (6)

No. of variant	1	2	3	4	5	6
M_1/M_0	0,670	0,707	0,742	0,775	0,806	0,837
s_1	0,4	0,6	0,6	0,6	0,5	0,588
s_2	0,6	1,2	1,4	1,45	1,576	1,6
K_1	50	75	75	45	137,5	26,25

for the given velocity distribution and values of P_{e0} and T_{e0}. Calculations showed that boundary-layer separation does not occur for variants 5 and 6 in Table 2 with P_{e0} = 1 atm, T_{e0} = 1500°K, and T_w = 373°K.

The number 3 in Fig. 2 denotes the corresponding nozzle contours for variant 6, while the data in Fig. 3a shows the distribution of m*(s) in this nozzle. In contrast to curves 1 and 2 (Fig. 3a), curve 3 has two maximums. Meanwhile, the first maximum from the left occurs as a result of the nonmonotonic nature of the function M(s) and is located in the neighborhood of its minimum (the minimum value of M is reached at $s = s_4$, noted in Fig. 3). At the same time, for the distributions determined by the parameters in the four left-most columns of Table 2, integration of the boundary-layer equations at a certain point near the velocity minimum produces an instability in the calculation, this instability being due to a change in sign at the value $\partial u/\partial n|_{n=0}$. This allows us to conclude that boundary-layer separation occurs at this point. If the condition $\partial u/\partial n|_{n=0} > 0$ were satisfied at all design points on the wall, as in the last two variants, the flow could be assumed intact.

It should be noted that the intactness of the flow in a compressible boundary layer with a given wall temperature also depends on the temperature of the inviscid flow [5]. Figure 3b shows the relation m*(s) for the distribution of M(s) corresponding to the set of parameters from variant 1 in Table 2 at T_{e0} equal to 4000 and 3000°K. It can be seen that the thickness of the boundary layer near the minimum of the function M(s) increases sharply with a decrease in T_{e0}. Boundary-layer separation occurs beginning with a certain value of T_{e0}. For example, the flow becomes separated at T_{e0} = 1500°K for the given distribution of M(s).

NOTATION

x, y, Cartesian coordinates; r_A, size of inlet aperture; s, coordinate directed along tangent to wall and dimensionless with respect to r_A; n, coordinate directed along normal to wall; ℓ, length of curve AB; L, length of curve AB dimensionless with respect to r_A; r(s), wall ordinate; V_x, V_y, projection of velocity vector onto x and y axes; u, v, projection of velocity vector in directions s and n; w, velocity modulus; θ, slope of velocity vector to x axis; M, Mach number; P, pressure; ρ, density; $\varkappa$, exponent of adiabatic curve; C_1 and C_2, constants in the Bernoulli and energy equations; h, total enthalpy of a unit mass; μ, viscosity coefficient; Pr, Prandtl number; R, gas constant. Indices: e, outer boundary of boundary layer; w, wall; 0, point A (Fig. 1).

LITERATURE CITED

1. I. L. Osipov, "Numerical method of designing plane nozzles," Izv. Akad. Nauk SSSR, Mekh. Zhidk. Gaza, No. 2, 179-183 (1979).
2. A. P. Byrkin and V. V. Shchennikov, "Numerical method of calculating a laminar boundary layer," Zh. Vychisl. Mat. Mat. Fiz., 10, No. 1, 124-131 (1970).
3. G.-G. Borger, "Optimierung von Windkanaldusen fur den Unterschallbereich," Z. Flugwiss., 23, No. 2, 45-50 (1975).
4. J. Anderson, Gas-Discharge Lasers [Russian translation], Mir, Moscow (1979).
5. G. Schlichting, Boundary Layer Theory, McGraw-Hill.